THE CONVERSION OF URANIUM HEXAFLUORIDE TO DIOXIDE

N. P. Galkin, U. D. Veryatin,
I. F. Yakhonin, A. F. Lugonov,
and Yu. M. Dymkov

UDC 621.039.59:621.039.543.6

The processing of uranium hexafluoride is considered in various publications, many of which deal with the production of oxides by high-temperature hydrolysis (pyrohydrolysis) [1-4]. Apart from methods that provide a powder, it is also possible to produce a granulated oxide directly by pyrohydrolysis [4-8]. In that case, the essence of the granulation is that the uranium dioxide obtained by reaction of the hexafluoride with a steam–hydrogen mixture grows on nuclei consisting also of uranium dioxide, which constitute the material in a fluidized bed.

A wide range was used for the molar ratio of the components: $UF_6:H_2O:H_2$ = 1:(2-12):(5-20); intermediate products are UF_4, U_3O_8, and UO_2F_2. In a fluidized bed, these are rapidly converted to uranium dioxide, the over-all pyrohydrolysis equation being

$$UF_6 + 2H_2O + H_2 = UO_2 + 6HF. \quad (1)$$

It was found during these studies that the ratio of the reagents substantially influences the characteristics of the final product. If there is a considerable excess of water vapor ($UF_6:H_2O$ = 7-12), one gets a large number of fine fractions in the granulated product, which have a low density, which is evidently due to the preferential formation of U_3O_8 in

$$3UF_6 + 9H_2O = U_3O_8 + 18HF + 0.5O_2. \quad (2)$$

The presence of oxygen allows UO_2 to be oxidized to U_3O_8, which reduces the particle size and density.

The technological process is divided into two stages in principle: pyrohydrolysis, which removes 97-99% of the fluorine, and final defluorination to a residual fluorine content less than 0.01 mass %. The hexafluoride is not supplied to the reaction vessel at this stage. A temperature of 600-650°C is adequate for the first stage, but 700-750°C is required for the second.

Further studies [9, 10] have facilitated the design of apparatus of two-chamber type, in which both stages are effected. In the pyrohydrolysis chamber, the hexafluoride is converted to dioxide, which grows on nuclei forming a fluidized bed. As the depth of the bed increases, the granules are transferred via a transfer line to the defluorination chamber, where a fluidized bed is used to remove the residual fluorine by means of a steam–hydrogen mixture.

The apparatus consists of the following units: a two-chamber pyrohydrolysis and defluorination reactor, a system for dispensing steam and gases, a hexafluoride evaporator, a system for condensing the excess of steam and hydrogen fluoride, and a system for burning the excess hydrogen. This apparatus has been used in making experimental batches of granulated uranium dioxide for loading in to vibroconsolidated fuel pins (Table 1). The process is monitored from the pressure difference Δp across the bed in the chamber, since the value of Δp is dependent on the grain-size composition. Experiments were performed with various throughputs (from 165 to 950 g/h) of uranium hexafluoride. The finished granules from the apparatus were submitted for sieve analysis, and the packed density and pycnometric density were determined fraction by fraction. Samples were taken from each fraction for chemical analysis (contents of uranium and fluorine), for x-ray analysis (lattice-parameter determination), spectral analysis (determination of impurities), and metallography.

It was found that the hexafluoride flow rate and the duration of the pyrohydrolysis affect the grain-size composition; an elevated rate (up to 1000 g/hr) leads to preferential growth of the fine fraction (−0.10 to +0.05 mm and less), while there is rapid enlargement of the larger particles (above 0.5 mm). The fine fraction is formed because of increase in

Translated from Atomnaya Énergiya, Vol. 52, No. 1, pp. 36-39, January, 1982. Original article submitted May 20, 1980.

0038-531X/82/5201-0045$07.50

TABLE 1. Technological Mode of Pyrohydrolysis of Uranium Hexafluoride (Load of Initial Uranium Dioxide 1500-2000 g)

UF_6 flow rate, g/h	Run time, h	Hydrolysis chamber				Defluorination chamber			Molar ratio UF_6:H_2O	Increase in mass of UO_2, g
		T,° C	p, kPa	Δp, kPa	Fluoridization argon flow, liter/h	T,° C	Δp, kPa	Volume ratio H_2O_{vap} : H_2		
240	5,0	610	8,0	5,3—7,5	1200	680	0—2,7	1 : 4	1 : 4 : 7	932
300	5,5	650	12,0	4,8—6,4	1000	700	0—3,2	1 : 6	1 : 6 : 6	1280
340	7,0	650	8,0	6,9—8,0	1000	700	0—3,2	1 : 11	1 : 4 : 6	1860
240	8,2	660	9,3	6,1—7,7	600	730	0—3,3	1 : 6	1 : 3 : 6	1514
165	5,0	660	5,3	7,2—8,5	600	700	0—2,8	1 : 4	1 : 2 : 5	642
430	2,5	660	5,3	6,9—7,5	600	720	0—2,1	1 : 5	1 : 3 : 7	844
240	8,0	650	5,3	7,2—9,1	600	700	0—9,1	1 : 4	1 : 3 : 5	1476
375	8,0	660	6,7	5,3—9,1	700	750	0—8,4	1 : 10	1 : 3 : 5	2340
272	7,0	610	5,3	2,8—8,3	700	750	0—6,7	1 : 8	1 : 3 : 5	1480
801	1,7	650	10,7	3,3—9,3	700	730	0—4,8	1 : 4	1 : 3 : 6	1035
950	1,5	650	22,6	5,6—6,4	800	740	0—4,2	1 : 4	1 : 2 : 3	1110

TABLE 2. Characteristics of the UO_2 Granulate Obtained with Pyrohydrolysis

Fraction number	Mass % of fraction in product	Equivalent diameter, mm		Fluorine content, mass %	Density, g/cm³	
		initial	final		packed	average
1	61,8					
2	37,6	0,33	0,40	0,009	6,3	10,6
3	0,6					
1	61,5					
2	34,0	0,31	0,38	0,012	6,1	10,3
3	4,5					
1	33,7					
2	61,6	0,27	0,37	0,003	6,3	10,3
3	4,7					
1	39,6					
2	55,0	0,30	0,32	0,009	6,2	10,4
3	6,4					
1	37,9					
2	55,0	0,27	0,32	0,009	6,2	10,4
3	7,2					
1	30,2					
2	60,8	0,26	0,28	0,003	6,2	10,4
3	9,0					
1	37,2					
2	56,1	0,24	0,26	0,009	6,4	10,5
3	6,7					
1	52,3					
2	41,5	0,29	0,37	0,005	6,0	10,4
3	6,2					
1	47,0					
2	42,5	0,22	0,26	0,02	6,4	10,4
3	10,5					
1	45,6					
2	43,5	0,27	0,23	0,02	5,6	10,1
3	10,9					
1	44,9					
2	38,9	0,37	0,22	0,01	5,8	10,0
3	16,2					

*The sizes of fractions 1-3 were −1.0 + 0.4; −0.4 + 0.1 and −0.1 + 0.5 mm.

the number of crystallization centers and the preferential production of new dioxide particles in the reaction volume.

At moderate flow rates (300-400 g/hr), there is uniform growth of the medium-sized granules (0.25-0.40 mm). The following molar ratio of the components was found to be optimal: $UF_6:H_2O:H_2 = 1:(3-6):(5-10)$.

Table 2 gives the physicochemical characteristics of the granules. In all experiments except two, the grain size increased (by comparison with the initial value). The products

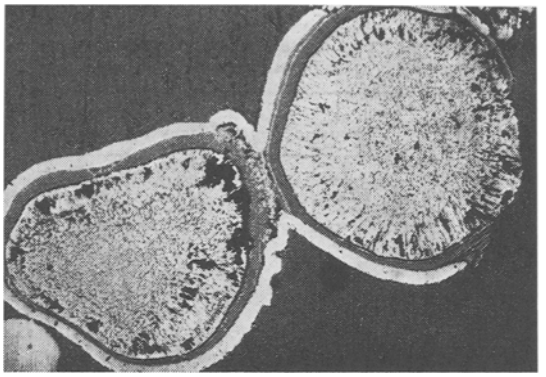

Fig. 1.

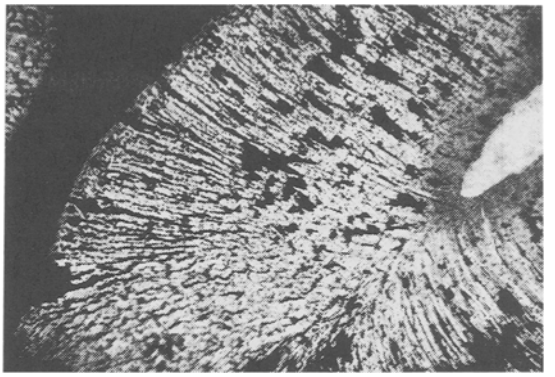

Fig. 2.

Fig. 1. Granules of highly anisotropic U_3O_8; photomicrograph of thin section (× 200).

Fig. 2. U_3O_8 spherulite forming around a uranium dioxide fragment. Photomicrograph of section (× 500).

from two experiments had relative high fluorine contents and reduced density, which was due to the elevated UF_6 flow rate and the corresponding instability in the fluidization. In the other experiments the product contained fluorine at the 0.001 level, while the density was 10.3-10.6 g/cm^3. Part of the granulated product was sintered at 1450°C under volume to reduce the residual fluorine content and raise the density.

Tests on the vibroconsolidated UO_2 in fuel-pin sheaths for a fast reactor were performed using an electrodynamic vibrator type VÉDS-200, and then the density of the fuel core was 8.8 + 0.2 g/cm^3. We measured the height of the consolidated column after vibroconsolidation and calculated the density of the core (Table 3). This density provided an important conclusion on the applicability of the granulate from pyrohydrolysis as a material for fuel pins.

Metallography was used to elucidate the phase transitions during the formation of the granules. The transitions between the phases were established in special experiments (Figs. 1-3). Light-field and dark-field metallography were applied to polished sections of the granules mounted in epoxide resin. We observed the dioxide, U_3O_8, and uranium tetrafluoride; in certain specimens there were microscopic inclusions of a phase whose relief and reflection were close to those of U_4O_9. Two-stage cellulose-carbon replicas from polished sections of the granules were etched with nitric acid and examined with a transmission electron microscope; the surfaces of the granules (after gold coating) were examined in a scanning electron microscope.

The formation conditions for granules leaving the reaction zone are different from those from granules within the fluidized bed (freely fluidized granules) because the processes in the granules that have left the bed occur more slowly, and the main metastable phases may persist to the end. The differences in reduction kinetics in the various zone of the reactor provide a full indication of the evolution of the reduction products and of the reactions of the hexafluoride with the seeds (uranium dioxide).

The following substitutions were observed: uranium tetrafluoride $\rightleftarrows$ U_3O_8; U_3O_8 $\rightleftarrows$ dioxide II (newly formed); dioxide I (seed) $\rightleftarrows$ U_3O_8; dioxide I $\rightleftarrows$ dioxide II. The tetrafluoride was observed as external fine-grained columnar shells surrounding and cementing granules of U_3O_8, and also as independent granules and spherulites.

U_3O_8 forms periodic textures showing sequential replacement or deposition in the tetrafluoride (Fig. 1). A eutectic structure between U_3O_8 and the tetrafluoride is also observed, and also signs of replacement of U_3O_8 by the tetrafluoride, which shows that there is an unstable equilibrium between UF_4 and U_3O_8, with repeated phase transitions. The UF_4 and U_3O_8 crystallize virtually simultaneously, with the crystallization front of UF_4 running ahead somewhat.

U_3O_8 accumulates in the intermediate pyrohydrolysis products. X-ray examination revealed two modifications of U_3O_8: the orthorhombic α modification with parameters a =

TABLE 3. Conditions and Results in Vibroconsolidation of Granulate

Vibrational frequency, Hz	Acceleration, g	Time, sec	Core density, g/cm³
1100	15	150	8,51
1100	30	120	8,48
1240	45—95	120	8,73
1400	40	80	9,01
1170	55—80	150	8,78
1170	50	70	9,11
1170	55	120	9,17
1170	50	120	8,97
1300	20	300	8,78
1300	20	85	8,85
1300	20	120	8,89

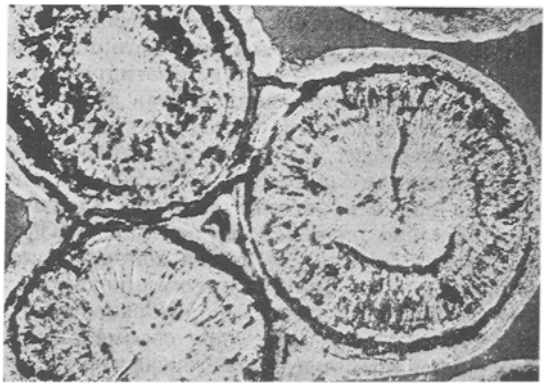

Fig. 3. Pseudomorphs of uranium dioxide after U_3O_8 spherulites. Photomicrograph (× 200).

(0.69 ± 0.01) kX; b = (3.983 ± 0.01) kX; c = (4.120 ± 0.005) kX and the modification U_3O_{8-x} with parameters a = (6.758 ± 0.01) kX; b = (4.064 ± 0.01) kX; c = (4.130 ± 0.05) kX, which are close to the parameters of $U_{11}O_{29}$ single crystals (composition $UO_{2.635}$).

A considerable fraction of the spherulites and granules of U_3O_8 may be formed around fragments of the dioxide (Fig. 2). The observations show that the uranium dioxide can replace the U_3O_8 spherulites completely. Many of the granules are pseudomorphs of UO_2 after U_3O_8 (Fig. 3), which retain all the structure details of the U_3O_8 protospherulites.

It seems that $U_3O_8 \rightleftarrows UO_2$ phase equilibrium occurs in the granules leaving the layer; these granules are unsymmetrical, which indicates deviations from all-round mass transfer. The transition of U_3O_8 to UO_2 may occur in stages during the reduction: $U_3O_8 \rightleftarrows U_3O_{8-x}$ $(U_8O_{21}) \rightarrow (U_4O_9) \rightarrow UO_{2+x} \rightarrow UO_2$. In the microscope one can distinguish the UO_{2+x} phase formed after U_3O_8, which is completely isotropic, but which has lower reflectivity than UO_2. The granular U_3O_8 aggregate and the dioxide occasionally contain small crystals of a uranium oxide whose reflectivity and hardness are somewhat higher than those of UO_2. It may be that this phase is U_4O_9 ($UO_{2.24}$).

Metallography confirmed these stages in the process via the tetrafluoride and U_3O_8. Uranyl fluoride is not observed in this way because of its solubility. The intermediate products are rapidly transformed to the dioxide that produces the final granules under the conditions of the vigorous mass transfer in the fluidized bed. Further research is needed to establish the presence and reasons for formation of U_4O_9, which can influence the oxygen coefficient of the final product (uranium dioxide).

LITERATURE CITED

1. S. Brandberg, Nucl. Technol., 18, No. 2, 177 (1973).
2. British Patent No. 1500790 (1975).

3. US Patent No. 3979499 (1976).
4. US Patent No. 3179499 (1965).
5. I. Knudsen et al., Trans. Am. Nucl. Soc., 5, No. 2, 335 (1962).
6. US Patent No. 3547598 (1970).
7. U. D. Veryatin and I. F. Yakhonin, Jad. Energ., 21, No. 7, 262 (1975).
8. N. P. Galkin et al., in: Proceedings of the Fourth COMECON Symposium [in Russian], Vol. 1, Karlovy Vary (1977), p. 282.
9. R. Aikhler et al., ibid., Vol. 2, p. 348.
10. H. Grünberg, in: Proceedings of the Third COMECON Symposium [in Russian], Vol. 1, Marianske Lazne (1975), p. 208.

METHODS OF CALCULATING RADIAL BOUNDARY CONDITIONS FOR FLUX TRAP CONTROL ASSEMBLIES

Frej Wasastjerna* and Eeva Koskinen†

Some methods of calculating a two- or four-group albedo matrix for the control assemblies of VVÉR-440 reactors are discussed. All of these methods use the S_N program DTF-IV to calculate partial neutron currents, but the group constants for the DTF-IV calculations were obtained by different methods. The influence of the boron steel absorber on the thermalization cross section of the water in the control assembly turned out to affect the albedo matrix significantly. The control assembly itself does not, however, have any significant effect on the group constants of adjacent fuel assemblies.

For fast control of VVER-440 reactors, flux trap control assemblies are used. These consist of an absorber part and a fuel follower. The absorber part essentially consists of a hexagonal tube of boron steel filled with water and some structural components of steel.

In Finland global reactor calculations of VVÉR-440 reactors are carried out using the two-dimensional two-group corase-mesh diffusion program HEXBU [1] or its three-dimensional counterpart HEXBU-3D [2]. In these programs the absorber part of a control assembly is represented by internal boundary conditions. This article will describe some methods of computing these boundary conditions, using computer programs available at the Nuclear Engineering Laboratory of the Technical Research Center of Finland. Only radial boundary conditions will be considered, though axial boundary conditions for use at the interface between the fuel follower and the absorber were also calculated in [3], as were boundary conditions for the outer surface of the core.

We give first a brief description of the programs used.

FOG [4] is a one-dimensional diffusion program.

THERMOS-OTA [5] is a modification of the well-known THERMOS program [6]. This program uses collision probability theory to calculate thermal neutron flux distributions (below 2.5265 eV) in one-dimensional slab or cylinder geometry.

FORM [7] is a FORTRAN version of the MUFT program. It calculates the fast (down to 0.625 eV) neutron spectrum for a fundamental mode of given buckling in a light water reactor fuel pin cell or a similar near-homogeneous system. Besides the neutron flux and current spectra, few-group cross sections are available as output.

*Technical Research Center of Finland, Nuclear Engineering Laboratory, P.O.B. 169, SF-00181, Helsinki 18, Finland.
†Imatran Voima Oy, Research Department, P.O.B. 138, SF-00101, Helsinki 10, Finland.

Published in Atomnaya Energiya, Vol. 52, No. 1, pp. 39-44, January, 1982. Original article submitted May 20, 1980.

0038-531X/82/5201-0049$07.50